DOI: 10.1002/((please add manuscript number))
Article type: Communication

Photodynamic Controls of Harmful Algal Blooms by an Ultra-efficient and Degradable AIEgen-based Photosensitizer

Qiang Yue, Xuewen He, Neng Yan, Sidan Tian, Chenchen Liu, Wen-Xiong Wang, Liang Luo* and Ben Zhong Tang**

((Optional Dedication))

Q. Yue, Dr. S. Tian, Prof. L. Luo
National Engineering Research Center for Nanomedicine
College of Life Science and Technology
Huazhong University of Science and Technology
Wuhan 430074, P. R. China
E-mail: liangluo@hust.edu.cn

Dr. X. He, C. Liu, Prof. B. Z. Tang
Department of Chemistry and Hong Kong Branch of Chinese National
Engineering Research Center for Tissue Restoration and Reconstruction
The Hong Kong University of Science & Technology
Clear Water Bay, Kowloon, Hong Kong, P. R. China
E-mail: tangbenz@ust.hk

Dr. N. Yan, Prof. W.-X. Wang
School of Energy and Environment, State Key Laboratory of Marine Pollution,
City University of Hong Kong, Kowloon, Hong Kong, P. R. China
E-mail: wx.wang@cityu.edu.hk

Keywords: harmful algal blooms, photodynamic therapy, aggregation-induced emission, photosensitizers, reactive oxygen species

Harmful algal blooms (HAB) have severe impacts on human health, aquatic ecosystems, and economy. There is still a lack of effective means to control the algal blooms. Herein, a positively charged photosensitizer with aggregation induced emission (AIE) characteristics, namely TVP-A, is reported for its super-efficient, cost-effective, and eco-friendly governance of HAB. TVP-A possesses a characteristically

high quantum yield of harvesting white light into reactive oxygen species (ROS). Attributed to its positive charges, TVP-A has good water solubility and can quickly adsorb onto algal cells floating on the water surface. It effectively triggers cell death through oxidative destruction of the nuclei and chloroplasts of algae. The extremely low effective concentration of TVP-A and the short irradiation time by natural light in removing algal blooms ensure its application at large scales under most weather conditions, without affecting other existing organisms. The slow but consistent self-degradation of TVP-A during the photodynamic controls of algal blooms avoids generating any environmental residues or secondary pollution to environmental systems. TVP-A thereby serves as an excellent candidate for the green governance of HAB, and this work represents a new paradigm for the development of efficient and degradable AIEgens for future environmental applications.

Harmful algal blooms, or HAB, refer to the rapid increase or accumulation in the population of algae as a result of eutrophication.[1] Large-scale outbreaks of HAB result in oxygen depletion and release of harmful toxins, consequently causing massive death of aquatic animals as well as bringing severe damage to aquatic ecology and economy every year. HAB has become a major global environmental problem, threatening freshwater and marine areas where human life depends on, and needs to be addressed urgently.[1a, 2]

A variety of physical and chemical methods have been used to control the HAB.[1b, 3] Physical methods including isolation, ultrasound, flocculation, and salvage are

effective for small ponds, but less so for treating large areas of water.[1b] Commercial chemicals such as copper sulfate and herbicides can be applied for large areas.[3a, 4] However, killing algae by copper ions is slow and affected by pH, alkalinity, ion conductivity, and comes with an environmental risk of heavy metal accumulation.[3, 4b] Herbicidal compounds show efficient control of HAB, but they unavoidably trigger secondary and persistent pollution, which greatly limits their uses in drinking or aquaculture waters.[2e, 3, 5] On the other hand, reactive oxygen species (ROS)-generating algaecides, such as chlorites and peroxides, are efficient,[6] biocompatible, [2e] and cost-effective, but they can induce non-specific toxicity to other aquatic organisms.[1b, 7] In addition, the short-lived active ingredients require repetitively applying algaecides in an unsustainable manner.[2e, 3a]

Photosensitizers that can catalytically produce ROS upon light irradiation have emerged as ideal candidates for the control of HAB. They have been widely used in the photodynamic therapy of cancers and bacterial or fungal infections, but their applications in HAB management are much less well known.[3a, 6b, 8] Drabkova et al. screened different photosensitizers for the growth inhibition of six green algae or cyanobacteria species, and only a few of them were effective to some algal species.[3a, 6b] Cationic photosensitizers are more effective than anionic photosensitizers in inhibiting algal growth, suggesting that the chemical structures of photosensitizers may be important in killing the algal cells.[9] These existing photosensitizers, however, still face problems such as inappropriate absorption wavelength, insufficient ROS production, and environmental residues. More importantly, conventional organic

small-molecule photosensitizers have limited solubility in water with aggregation-caused quenching of fluorescence, limiting further fluorescence imaging-based investigation of photosensitizer-algal cell interactions.[10]

In recent years, photosensitizers with aggregation-induced emission (AIE) characteristics have been extensively studied in the field of biomedical diagnosis and therapy, attributing to their excellent fluorescence properties and ROS quantum yields at high concentrations or the state of aggregation. AIE luminogens (AIEgens) which can harvest white light for efficient ROS generation are particularly favorable to inhibit the algal blooms under natural conditions. In addition, the exceptional fluorescence imaging property of AIEgens in the aggregation state can also enable mechanistic study.[11] Herein, we developed a degradable, bright water-soluble AIEgen with ultra-high ROS quantum yield, namely TVP-A, that can effectively inhibit the algal growth and control their blooms under natural light illumination conditions (**Figure 1**A). TVP-A has good water solubility, and generates ROS with a high quantum yield upon exposure to natural light, making it possible to treat a wide variety of algae with high efficiency. More strikingly, it self-degrades gradually under natural conditions, so that it will not cause any harmful residue or secondary pollution to ecological systems. With the help of its excellent AIE characteristics, we also elucidated the process and mechanism of killing the algal cells by TVP-A, providing new insights into designing next generation of algaecides for green HAB governance.

TVP-A has a donor-acceptor (D-A) structure comprising moieties of triphenylamine (D), carbon-carbon double bond (π-bridge), and pyridinium (A, Figure 1A). In

addition, we have introduced a primary amino group onto the terminal pyridinium to further increase the solubility and make the compound positively charged. The synthesis and characterization of TVP-A are shown in Figures S1–S4 in the Supporting Information. The free rotation of the donor and acceptor moieties consumes the energy of excitons during excitation, resulting in no/weak fluorescence of the molecule in the dissolved state, whereas restricting these intramolecular rotations in the aggregated state or by steric hindrance can block the nonradiative decay and activate the strong fluorescence of the molecule.[11c, 12] The dual positively charged pyridinium and ammonium groups on TVP-A endows the molecule a good water solubility of as high as 2 mg mL^{-1}, allowing for reduced precipitation loss during massive spraying and increased efficiency in many subsequent aqueous applications that are difficult for other insoluble photosensitizers. Meanwhile, the positive charges also help the molecule readily attach to the negatively charged cell membrane of the algae, therefore implementing the PDT process for efficient removal of algal blooms.

The maximal absorption peak of TVP-A in water, centered at 460 nm, had a wide absorption range from 300 to 600 nm (Figure S5, Supporting Information), matching well with the solar radiation spectrum.[13] The measured aqueous molar absorption coefficient (ε) of TVP-A at 460 nm was 2.6×10^4 L mol^{-1} cm^{-1}. The fluorescence of TVP-A was very weak in water, with an almost undetectable fluorescence quantum yield (QY) of 0.27% (Table S1, Supporting Information). However, when an organic solvent such as tetrahydrofuran (THF) was present, the fluorescence signal of TVP-A

was gradually enhanced with the increased fraction of THF (Figure 1B,C). The fluorescence QY of TVP-A increased by about 40 times to 11.6% in pure THF. Moreover, the amphiphilic structure of TVP-A enabled its insertion into the hydrophobic regions of biological macromolecules such as proteins and cell membranes, where the increased steric hindrance led to restricted movement of TVP-A molecules and enhanced fluorescence emission (Figure 1D, Figure S6, Supporting Information). The value of QY of TVP-A (30.73%) in the bovine serum albumin (BSA) aqueous solution was boosted by nearly 100 times of that in pure water, making it possible to track the diffusion and distribution of TVP-A molecules in algal cells by fluorescence imaging. TVP-A herein represented a bright water-soluble fluorescent molecule with excellent AIE properties.

The integration of D-A structure and extension of π-conjugation further promoted intramolecular charge transfer (ICT), and decreased the energy gap between the lowest excited singlet state (S_1) and the lowest triplet state (T_1) through the highest occupied molecular orbitals (HOMO)–lowest unoccupied molecular orbitals (LUMO) separation, facilitating the generation of ROS.[11c, 14] To evaluate the ROS generation of TVP-A, we employed Rose Bengal (RB), a white light-absorbing commercial photosensitizer, as the reference.[14a, 15] It should be noted that photosensitizers usually generate more than one species of ROS,[16] and the effects of different types of ROS are variable under different conditions. For example, production of singlet oxygen ($^1O_2$) is usually the main focus in photodynamic cancer therapy,[8a, 14a, 17] whereas cyanobacteria are more sensitive to hydroxyl radicals (•OH), and green algae are more

sensitive $^1O_2$.[6b] Therefore, photosensitizers simultaneously producing multiple types of ROS hold great promise in their applications in complex environment of algal blooms formed by different algae. Here we used four different ROS probes to evaluate the generation of various types of ROS by TVP-A, including 2',7'-dichlorofluorescein diacetate (DCF-DA) for total ROS,[18] 9,10-anthracenediyl-bis(methylene)dimalonic acid (ABDA) for $^1O_2$,[14a] dihydrorhodamine 123 (DHR) for superoxide radicals ($O_2^{\bullet-}$),[19] and 2-[6-(4-hydroxy)phenoxy-3H-xanthen-3-on-9-yl]benzoic acid (HPF) for •OH.[20] All ROS tests were performed under the same white light irradiation conditions (1 mW cm^{-2}, 350-800 nm). Figure 1E showed that the fluorescence signals of DCF-DA increased promptly with irradiation time, indicating the efficient generation of ROS by TVP-A. Surprisingly, the increase rate of the fluorescence signal of the DCF-DA probe in the TVP-A aqueous solution was 10 times faster than that in the RB solution (Figure 1F, 1G), implying that TVP-A had an extremely high total ROS conversion rate. Further studies revealed that TVP-A was efficient in generating all three typical types of ROS upon white light irradiation. For TVP-A, the production efficiency of $^1O_2$ was almost equal to RB (Figure S7, Supporting Information), while that of $O_2^{\bullet-}$ was slightly less efficient than RB (Figure S8, Supporting Information), and the production rate of •OH was significantly higher than RB (Figure S9, Supporting Information). The superb generation efficiency of ROS, especially •OH, under white light irradiation indicated the great potential of TVP-A in treating HAB under natural conditions.

Most HAB are mainly caused by prokaryotic cyanobacteria and eukaryotic algae,

such as green algae.[2a, 2e, 3a] As a proof of concept, we selected one cyanobacteria (*Microcystis aeruginosa*, or *M. aeruginosa*) and two freshwater green algae (*Chlorella. vulgaris*, or *C. vulgaris*, and *Chlamydomonas reinhardtii*, or *C. reinhardtii*).[21] In this work, we used 16 h light (50 μEinstein m^{-2} s^{-1})/8 h dark cycles to simulate the daily change of natural light illumination and darkness. In order to explore the effective concentrations of TVP-A in controlling the algal blooms, we first cultured these algal cells until their cell density reached a level similar to the algal blooms (~1.5 × 10^7 cells mL^{-1}), followed by co-incubating them with TVP-A at different concentrations (0, 0.2, 0.5, 1.0, 2.5, 5.0 and 10.0 ppm) for 96 hours under the simulated light/dark daily cycles. The 50% effective concentration (EC_{50}) value of TCP-A was 0.45 ppm for *M. aeruginosa*, 0.85 ppm for *C. vulgaris*, and 0.84 ppm for *C. reinhardtii* (**Figure 2**A), respectively. The relatively lower EC_{50} of TVP-A for *M. aeruginosa* indicated that cyanobacteria were more sensitive to ROS, especially •OH, than the two eukaryotic cells, consistent with the previous studies.[6a, 6b]

We next compared the effectiveness of TVP-A with a commercial algaecide (Alg) in algal bloom control. As shown in Figure 2B, the algae *C. reinhardtii* (1.6 × 10^7 cells mL^{-1}) alone (control) continued to grow with adequate nutrients, rich light, and proper temperature over 5 days. Applying 10 ppm of Alg failed to remove the bloom within 5 days. A concentration as high as 100 ppm of Alg still resulted in incomplete clearance of algal cells. Strikingly, only 5 ppm of TVP-A was effective in removing the algal bloom after 5 simulated natural daily cycles. At 10 ppm of TVP-A, water restored to clear color during the testing period, suggesting the superior capacity of TVP-A in

algal bloom removal.

Figure 2C-E compiled the quantitative comparison between TVP-A and Alg in removing the blooms of all three algae, with the initial algal cell density simulating the bloom conditions. In the control samples without addition of TVP-A or Alg, the algal cell density of all three algae remained unchanged during the 5-day period. After adding 10 ppm of Alg, around 5% of the initial algal cells remained alive after 5 days, which was further reduced to around 1% of the initial values on Day 5 when 100 ppm of Alg was added. As a comparison, only 5 ppm of TVP-A was able to reduce the algal density to around 1% of the initial values on Day 5 under simulated daily cycling, displaying the comparable effectiveness as 100 ppm of Alg. The ability to quickly and efficiently eliminate algal blooms under extremely low working concentrations endowed TVP-A a great potential in treating large-scale algal blooms. In addition, we also evaluated the capability of TVP-A in preventing the occurrence of algal blooms (Figure 2F-H). At a low initial density of algal cells (around 5.0×10^5 cells mL^{-1} for all three algae), the algae in the control group increased by more than 20 times and reached a stationary phase within 5 days. The growth of all algal cells was effectively inhibited when treated with 5 ppm of TVP-A or 100 ppm of Alg, showing the exceptional preventing effect of TVP-A on the outbreak of algal blooms. Collectively, TVP-A could effectively inhibit the algal blooms at concentrations significantly lower than those of commercial algaecide Alg, exhibiting ultra-efficient controls of HAB.

To better understand the excellent removing effect of TVP-A on algal blooms, we

further explored the detailed mechanisms of killing algal cells by photodynamic treatment. *C. reinhardtii* was used as a model alga for subsequent experiments, because of their relatively large size and good dispersity. We monitored the zeta potential on the surface of the algal cells before and after incubation with TVP-A (Figure S10, Supporting Information). The mean surface zeta potential of the pristine algal cells was -33.03 mV, confirming the negatively charged nature of algal cell membranes. This value then changed to -25.95 mV immediately after TVP-A was added in the dark, implying that the positively charged TVP-A molecules were electrostatically adsorbed onto the algal cells. The zeta potential gradually increased with the extension of dark incubation, and reached -13.85 mV after 1 hour, proving the continuous accumulation of TVP-A on the algal surface. Further experiments were performed to investigate the effects of TVP-A (5 ppm) on the morphology of algal cells after continuous adsorption and irradiation by simulated natural light using scanning electronic microscopy (SEM).[22] As shown in **Figure 3**A, the normal algal cells appeared plump and spherical, but most algal cells were severely damaged or even collapsed after 2 h of photodynamic treatment by TVP-A (yellow box area of Figure 3A), confirming that photodynamic treatment by TVP-A could destruct the morphological and cytoskeleton structural integrity of algal cells.

The excellent AIE characteristics of TVP-A enabled us to track the internalization of TVP-A molecules in algal cells as well as their cellular distribution using confocal laser scanning microscopy (CLSM). Once *C. reinhardtii* and TVP-A (5 ppm) were mixed, the samples were immediately exposed to simulated natural light illumination

from 0 min to 10 min. CLSM images of the algal cells were taken after the mixture was centrifuged, washed, and re-suspended (Figure 3B). The CLSM images clearly illustrated the efficient uptake of TVP-A molecules in the algal cells. The fluorescence signals of TVP-A (green channel) were significantly enhanced when the molecules were bound with cellular biomacromolecules due to AIE (Figure 1D, Figure S6, Supporting Information), and mainly distributed in the algal cytoplasm after endocytosis. They were not overlapped with the signals of chlorophyll (red channel) or nucleic acid dye DAPI (blue channel) before being exposed to light irradiation (Figure 2B, 0 min). The morphologies of the nucleus and chloroplast were kept intact before photodynamic treatment. After 10 min under simulated natural light irradiation, the bright field CLSM images revealed an apparent plasmolysis (red arrow in Figure 3B), which unambiguously indicated the destruction of the cytoplasmic membrane.[23] The morphologies of the nucleus and chloroplast were destroyed with an attenuation of their fluorescence intensities, suggesting that these organelles were damaged after the photodynamic treatment. More interestingly, the fluorescence signals of TVP-A diffused over the whole algal cell, with a 97% overlap with the nucleus and a 99% overlap with the chloroplast (10 min, Figure 3B). The infiltration of the TVP-A molecules implied that the membrane structures of the algal cells were all destroyed during the photodynamic treatment. The diffused TVP-A molecules, on the other hand, might further accelerate the photodynamic destruction of biological structures inside the cells. In contrast, the integral structure of algal cells was unimpaired in the absence of natural light illumination, even under incubation with TVP-A for up to 120

min (Figure S11, Supporting Information), which confirmed that the cytotoxicity of TVP-A was mainly induced by light irradiation and ROS generation.

In order to further verify the irreversible destruction of chloroplast caused by the photodynamic treatment, we measured the change of chlorophyll fluorescence in *C. reinhardtii* (1.6×10^7 cells mL^{-1}) in the presence and absence of 5 ppm of TVP-A as a function of simulated natural light irradiation time. As shown in Figure 3C, D and Figure S12 (Supporting Information), the chlorophyll fluorescence intensity decreased by almost 50% after the cells were exposed to the illumination for only 5 min. The fluorescence intensity of chlorophyll decreased to < 20% and 4.3% after 2 and 24 h of illumination, respectively, whereas the fluorescence signals of TVP-A only decreased slightly during the same period, suggesting that TVP-A could constantly generate ROS in the PDT process. Chloroplast is a plastid in green plant cells in which photosynthesis takes places, and chlorophyll is a key component of photosynthesis.[5a] TVP-A was able to irreversibly and rapidly destroy these important organelles of algal cells at extremely low working conditions upon natural light irradiation, explaining its ultra-efficient elimination of algal blooms by photodynamic treatment. In addition, when the algae and TVP-A mixture were exposed to the simulated natural light illumination for 2 min and switched back to dark for another 24 h, almost all cells died along with cracked cell membranes and diminished chlorophyll fluorescence (Figure S13, Supporting Information). No plasmolysis was observed, suggesting that the cell death might be triggered by different mechanisms under this condition. Nevertheless, it took only 2 min of natural light irradiation for TVP-A to effectively

kill the algal cells, suggesting that this powerful method was applicable in most weather conditions for highly efficient bloom governance.

An ideal algaecide should not cause secondary pollution by generating environmental residues or hurting other aquatic plants and animals. We had observed that the color of TVP-A disappeared after treating the algae for several days (Figure 2B), suggesting that the photosensitizer might degrade itself under natural conditions. We also monitored the UV/vis absorption spectroscopic changes of the TVP-A aqueous solution (5 ppm) and the TVP-A THF suspension (5 ppm), respectively (**Figure** 4A-C). In these experiments we used a high-power white light lamp (350-800 nm, 10 mW cm^{-2}), in order to complete the experiments before the THF evaporation. In general, the absorbance of TVP-A decreased promptly upon high-power white light irradiation, indicating the rapid photo-bleaching of TVP-A under high energy irradiation. Interestingly, the degradation rate of TVP-A in THF was faster than that in water, suggesting that TVP-A was less resistant to degradation in the aggregation state. When 5 ppm of TVP-A was co-incubated with *C. reinhardtii* (5.0×10^5 cells mL^{-1}), the absorbance of TVP-A diminished gradually under the simulated natural light irradiation (Figure 4D,F), suggesting that TVP-A itself might degrade completely while clearing the algal cells without environmental residues. However, under dark conditions, TVP-A was much more stable except for an obvious degradation within the first day, which was possibly caused by ROS generation by algal metabolism.[24] Since most algal cells were killed within the first day, the degradation of TVP-A ceased afterwards accordingly.

To investigate the effects of TVP-A molecules on aquatic organisms other than algae, we designed a simple microcosm, which contained TVP-A (0 or 10 ppm), *C. reinhardtii* (5×10^4 mL^{-1}), freshwater medaka fish (*Oryzias latipes*, or *O. latipes*), fish bait, and filtered creek water (suitable for culturing of freshwater aquatic organisms [25]) in 250 ml flasks. After 14 days of cultivation under simulated daily cycles, few algal cells in the TVP-A containing microcosm were detectable, and the color of TVP-A also disappeared. More importantly, the fish remained healthy after the photodynamic treatment of algae (Figure 4G). There was no significant difference in the daily heart rates of the fish between the groups with and without TVP-A during the whole experimental period (Figure 4H), confirming the biocompatibility of TVP-A within the working concentration for algae treatment. We also evaluated the dark toxicity of TVP-A to normal mammalian tissue cells, and TVP-A showed negligible toxicity to human umbilical cord vein endothelial cells within the concentration range applying to algal blooms governance (Figure S14, Supporting Information).

In summary, we have for the first time designed and synthesized a new AIEgen-based photosensitizer TVP-A that can specifically kill algal cells and control the algal blooms with ultra-high efficiency. TVP-A possesses positive charges and super-efficient ROS production upon natural light irradiation, and effectively triggers oxidative destruction to the nuclei and chloroplasts of algae. The extremely low effective concentration of TVP-A and short irradiation time in removing the algal blooms ensure its application at large scales under most weather conditions, without affecting other organisms. The slow but consistent self-degradation of TVP-A during

the photodynamic governance of algal blooms results in no environmental residues or secondary pollution. TVP-A therefore represents a new AIE-based photosensitizer that can suppress the undesired algal blooms in a super-efficient, cost-effective, yet eco-friendly manner, shedding new light in developing next generation of algaecides for green governance of large-scale algal blooms.

Supporting Information

Supporting Information is available from the Wiley Online Library or from the author.

Acknowledgements

Qiang Yue, Xuewen He and Neng Yan contributed equally to this work. All authors discussed the results and commented on the paper. This work is supported by the National Natural Science Foundation of China (21877042), and the Huazhong University of Science and Technology Startup Fund for Young Talents. The authors acknowledge funding to B.Z.T. from the Research Grants Council of Hong Kong (C6009-17G), the Innovation and Technology Commission (ITC-CNERC14SC01), the National Natural Science Foundation of China (21788102), and the National Key Research and Development program of China (2018YFE0190200). We also thank Prof. Jianglin Wang of Huazhong University of Science and Technology for help on mammalian cells.

Received: ((will be filled in by the editorial staff))
Revised: ((will be filled in by the editorial staff))
Published online: ((will be filled in by the editorial staff))

References

[1] a) E. B. I. R.M. Kudela (UCSC), CSIC), S. Bernard (CSIR-NRE), M. Burford (ARI-UG), L. Fernand (CEFAS), S. Lu (JU), S. Roy (UQAR), P. Tester (NOAA), G. Usup, R. M. N. (UKM), D. M. Anderson (WHOI), A. Cembella (AWI), M. Chinain, G. H. U. (ILM), B. Reguera (IEO), A. Zingone (SZN), H. Enevoldsen (IOC), Ed, U. (SCOR). *IOC/UNESCO* **2015**; b) J. J. Gallardo-Rodríguez, A. Astuya-Villalón, A. Llanos-Rivera, V. Avello-Fontalba, V.

Ulloa-Jofré, *Rev Aquac.* **2019**, *11*, 661-684.

[2] a) J. C. Ho, A. M. Michalak, N. Pahlevan, *Nature.* **2019**, *574*, 667-670; b) M. Qu, D. D. Lefebvre, Y. Wang, Y. Qu, D. Zhu, W. Ren, *Science.* **2014**, *346*, 175-176; c) A. M. Michalak, E. J. Anderson, D. Beletsky, S. Boland, N. S. Bosch, T. B. Bridgeman, J. D. Chaffin, K. Cho, R. Confesor, I. Daloğlu, J. V. DePinto, M. A. Evans, G. L. Fahnenstiel, L. He, J. C. Ho, L. Jenkins, T. H. Johengen, K. C. Kuo, E. LaPorte, X. Liu, M. R. McWilliams, M. R. Moore, D. J. Posselt, R. P. Richards, D. Scavia, A. L. Steiner, E. Verhamme, D. M. Wright, M. A. Zagorski, *PNAS.* **2013**, *110*, 6448-6452; d) H. W. Paerl, W. S. Gardner, M. J. McCarthy, B. L. Peierls, S. W. Wilhelm, *Science.* **2014**, *346*, 175-175; e) J. Huisman, G. A. Codd, H. W. Paerl, B. W. Ibelings, J. M. H. Verspagen, P. M. Visser, *Nat. Rev. Microbiol.* **2018**, *16*, 471-483; f) W. A. Wurtsbaugh, H. W. Paerl, W. K. Dodds, *Wiley Interdiscip. Rev. Water.* **2019**, *6*.

[3] a) D. Jancula, B. Marsalek, *Chemosphere* **2011**, *85*, 1415-1422; b) H. C. P. Matthijs, D. Jančula, P. M. Visser, B. Maršálek, *Aquatic Ecol.* **2016**, *50*, 443-460.

[4] a) S. Zhou, Y. Shao, N. Gao, Y. Deng, J. Qiao, H. Ou, J. Deng, *Sci. Total Environ.* **2013**, 463-464, 111-119; b) E. J. Rounsefell GA, U.S. Fish and Wildlife Service Special Scientific Report – Fisheries, No. 270. U.S. Department of the Interior, Fish and Wildlife Service, Washington, DC. **1958**.

[5] a) G. Sadhasivam, C. Gelber, V. Zakin, S. Margel, O. H. Shapiro, *Environ.Sci. Technol.* **2019**, 53, 9160-9170; b) S. Giacomazzi, N. Cochet, *Chemosphere*.

2004, 56, 1021-1032; c) J. A. Field, R. L. Reed, T. E. Sawyer, S. M. Griffith, J. P. J. Wigington, *J. Environ.Qual.* **2003**, 32, 171-179.

[6] a) M. Drábková, W. Admiraal, B. Maršálek, *Environ.Sci. Technol.* **2007**, *41*, 309-314; b) M. Drabkova, B. Marsalek, W. Admiraal, *Environ.Toxicol.* **2007**, *22*, 112-115; c) H. C. Matthijs, P. M. Visser, B. Reeze, J. Meeuse, P. C. Slot, G. Wijn, R. Talens, J. Huisman, *Water Res.* **2012**, *46*, 1460-1472.

[7] J. A. Zillich, *J Water Pollut Control Fed.* **1972**, *44*, 211-220.

[8] a) M. Lan, S. Zhao, W. Liu, C. S. Lee, W. Zhang, P. Wang, *Adv. Healthc.Mater.* **2019**, *8*, e1900132; b) Q. Chen, H. Dan, F. Tang, J. Wang, X. Li, J. Cheng, H. Zhao, X. Zeng, *Int. J. Oral .Sci.* **2019**, *11*, 14; c) L. Huang, Y. Xuan, Y. Koide, T. Zhiyentayev, M. Tanaka, M. R. Hamblin, *Lasers Surg Med.* **2012**, *44*, 490-499.

[9] a; bJ. Pohl, I. Saltsman, A. Mahammed, Z. Gross, B. Roder, *J. Appl. Microbiol.* **2015**, *118*, 305-312.

[10] a) M. Li, Y. Gao, Y. Yuan, Y. Wu, Z. Song, B. Z. Tang, B. Liu, Q. C. Zheng, *ACS nano.* **2017**, *11*, 3922-3932; b) N. Sekkat, H. van den Bergh, T. Nyokong, N. Lange, *Molecules.* **2011**, *17*, 98-144; c) Y. Yuan, C.-J. Zhang, B. Liu, *ChemComm.* **2015**, *51*, 8626-8629.

[11] a) Y. Hong, J. W. Y. Lam, B. Z. Tang, *ChemComm.* **2009**, 4332-4353; b) F. Hu, S. Xu, B. Liu, *Adv. Mater.* **2018**, *30*, e1801350; c) J. Mei, N. L. Leung, R. T. Kwok, J. W. Lam, B. Z. Tang, *Chem. Rev.* **2015**, *115*, 11718-11940.

[12] X. He, Y. Yang, Y. Guo, S. Lu, Y. Du, J.-J. Li, X. Zhang, N. L. C. Leung, Z.

Zhao, G. Niu, S. Yang, Z. Weng, R. T. K. Kwok, J. W. Y. Lam, G. Xie, B. Z. Tang, *J. Am. Chem. Soc.* **2020**, *142*, 3959-3969.

[13] J. Skupin, S. Noël, M. W. Wuttke, M. Gottwald, H. Bovensmann, M. Weber, J. P. Burrows, *Adv. Space Res.* **2005**, *35*, 370-375.

[14] a) Y. Gao, X. Wang, X. He, Z. He, X. Yang, S. Tian, F. Meng, D. Ding, L. Luo, B. Z. Tang, *Adv. Funct. Mater.* **2019**, *29*, 1902673; b) D. Wang, M. M. S. Lee, G. Shan, R. T. K. Kwok, J. W. Y. Lam, H. Su, Y. Cai, B. Z. Tang, *Adv. Mater.* **2018**, *30*, e1802105.

[15] Y. Zhang, X. Zhao, Y. Li, X. Wang, Q. Wang, H. Lu, L. Zhu, ***Dyes** Pigm.* **2019**, *165*, 53-57.

[16] Y. Nosaka, A. Y. Nosaka, *Chem. Rev.* **2017**, *117*, 11302-11336.

[17] a) W. Wu, D. Mao, F. Hu, S. Xu, C. Chen, C. J. Zhang, X. Cheng, Y. Yuan, D. Ding, D. Kong, B. Liu, *Adv. Mater.* **2017**, *29*; b) Y. Zheng, H. Lu, Z. Jiang, Y. Guan, J. Zou, X. Wang, R. Cheng, H. Gao, *J Mater Chem B.* **2017**, *5*, 6277-6281.

[18] A. Gomes, E. Fernandes, J. L. Lima, *J Biochem Biophys Methods.* **2005**, *65*, 45-80.

[19] L. M. HENDERSON, J. B. CHAPPELL, *Eur J Biochem.* **1993**, *217*, 973-980.

[20] K. Setsukinai, Y. Urano, K. Kakinuma, H. J. Majima, T. Nagano, *J. Biol. Chem.* **2003**, *278*, 3170-3175.

[21] aH. Song, M. Lavoie, X. Fan, H. Tan, G. Liu, P. Xu, Z. Fu, H. W. Paerl, H. Qian, ***ISME** J.* **2017**, *11*, 1865-1876; bR. R. L. Guillard, C. J. Lorenzen, *J. Phycol.* **1972**, *8*, 10-14.

[22] C. Zhang, X. Chen, J. Wang, L. Tan, *Environ.Pollut.* **2017**, *220*, 1282-1288.

[23] D. K. Khona, S. M. Shirolikar, K. K. Gawde, E. Hom, M. A. Deodhar, J. S. D'Souza, *Algal Res.* **2016**, *16*, 434-448.

[24] C. Triantaphylidès, M. Krischke, F. A. Hoeberichts, B. Ksas, G. Gresser, M. Havaux, F. Van Breusegem, M. J. Mueller, *Plant Physiol.* **2008**, *148*, 960-968.

[25] N. Yan, X. He, B. Z. Tang, W. X. Wang, *Environ. Sci. Technol.* **2019**, *53*, 5895-5905.

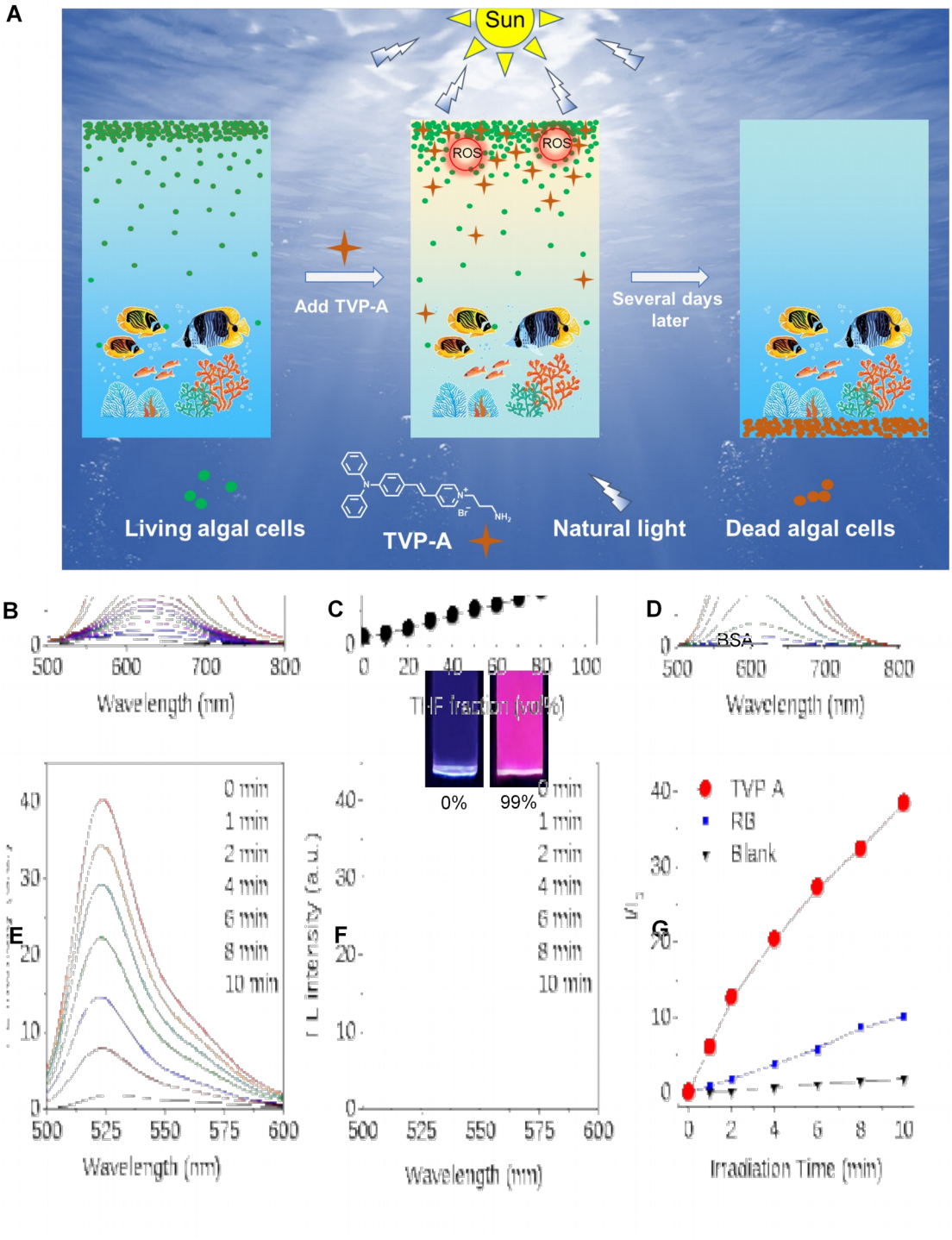

Figure 1. (A) Schematic illustration of selectively removing algal blooms by TVP-A upon natural light irradiation. (B) Fluorescence (FL) spectra of TVP-A (20 μM, λ_{ex} = 488 nm) in H_2O/THF mixed solvents with various fractions of THF. Inset: Pictures of TVP-A aqueous solutions containing 0% and 99% THF. (C) Relative FL intensity of TVP-A at 625 nm as a function of the THF fraction, where I_0 is the FL intensity of TVP-A aqueous solution with 0% THF. (D) FL spectra of TVP-A aqueous solutions in the presence of different concentrations of BSA (from 0 to 1200 μg/mL). Inset: FL intensity of TVP-A at 607 nm versus concentrations of BSA. E) FL spectra of DCF-

DA (10 μM, λ_{ex} = 488 nm) in a TVP-A aqueous solution (5 μM) irradiated by white light (350-800 nm, 1 mW cm^{-2}) for different time. F) FL spectra of DCF-DA (10 μM, λ_{ex} = 488 nm) in a RB aqueous solution irradiated by white light (350-800 nm, 1 mW cm^{-2}) for different time. G) FL intensity of DCF-DA at 524 nm in blank, TVP-A (5 μM), and Rose Bengal (5 μM) aqueous solutions upon white light irradiation for different time.

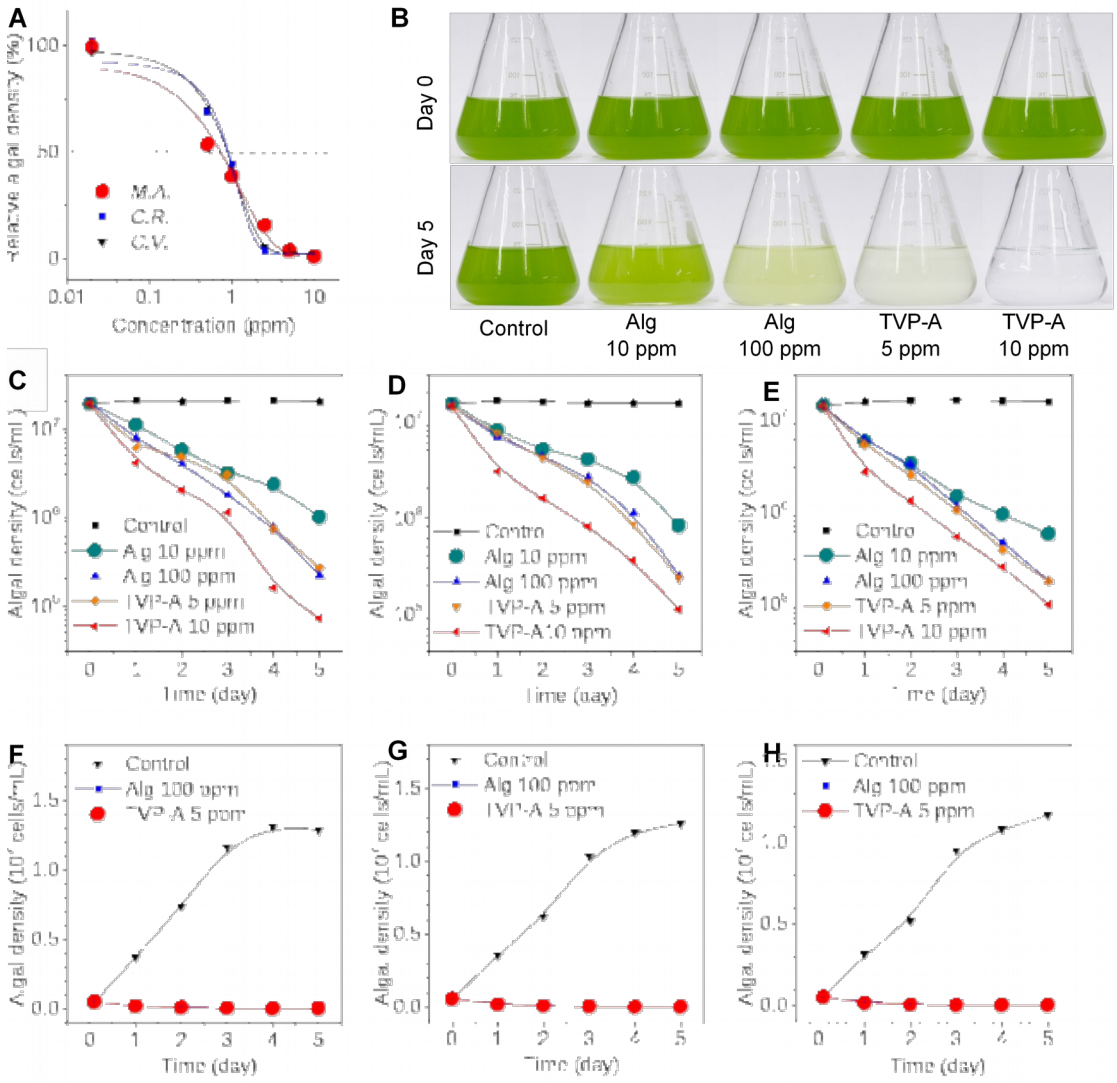

Figure 2. (A) Relative cell density of three algae in the presence of TVP-A at different concentrations after 96 hours under the simulated daily cycles. *M.A.*: *M. aeruginosa*; *C.R.*: *C. reinhardtii*; *C.V.*: *C. vulgaris*. (B) Pictures of *C. reinhardtii* (1.6×10^7 cells mL^{-1}) on Day 0 and Day 5 in the presence of Alg or TVP-A with different concentrations under the simulated daily cycles. (C-E) Dose-dependent killing effect of TVP-A (under the simulated daily cycles) and Alg on removing blooms caused by *M. aeruginosa* (C), *C. reinhardtii* (D), and *C. vulgaris* (E). The inhibition effect of TVP-A (under the simulated daily cycles) and Alg on the growth of *M. aeruginosa* (F), *C. reinhardtii* (G) and *C. vulgaris*(H). Simulated daily cycle: 16 h light (50 μEinstein m^{-2} s^{-1})/8 h dark.

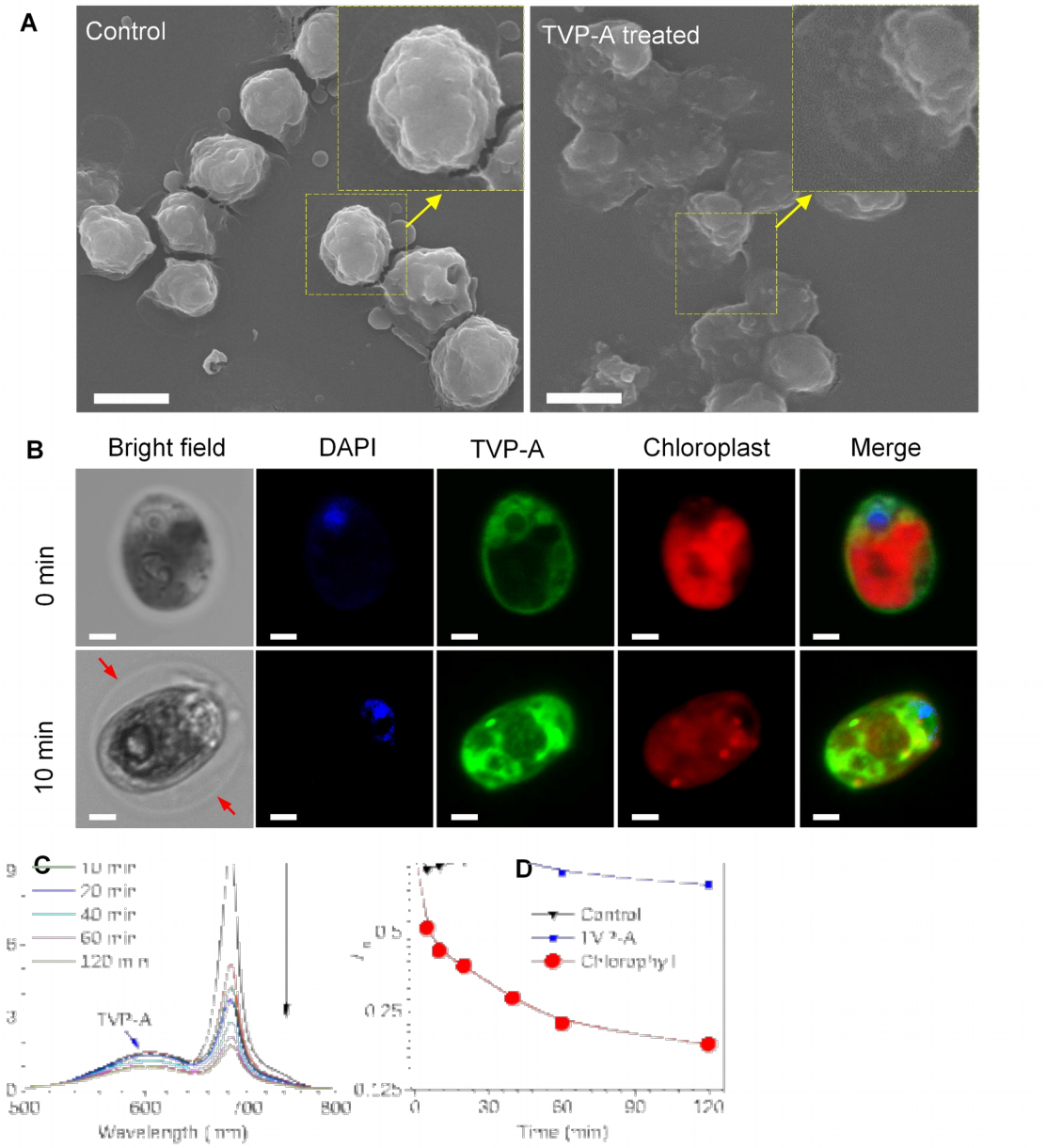

Figure 3. (A) SEM images of control and TVP-A treated (5 ppm, 2 h of simulated natural light illumination) *C. reinhardtii* (5.0×10^6 cells mL^{-1}). Scale bar: 10 μm. (B) CLSM images of a *C. reinhardtii* cell co-incubated with TVP-A (5 ppm) and irradiated by simulated natural light for 0 and 10 min. TVP-A: green channel, λ_{ex} = 488 nm, λ_{em} = 570-630 nm; Chlorophyll: red channel, λ_{ex} = 405 nm, λ_{em} = 670-700 nm; DAPI: blue channel, λ_{ex} = 405 nm, λ_{em} = 450-500 nm. Scale bar: 2 μm. (C) FL spectra of *C. reinhardtii* algal cells (1.6×10^7 cells mL^{-1}) in the presence of TVP-A (5 ppm) with different time of simulated natural light illumination. λ_{ex} = 488 nm. (D) The relative FL intensity at 600 nm (blue line, FL of TVP-A) and 682 nm (red line, FL of

chlorophyll) in (C) as a function of simulated natural light illumination time. The black line shows the change of FL intensity at 682 nm of a controlled algae solution without TVP-A. I_0 is the FL intensity of the corresponding sample with 0 min of illumination. Simulated natural light illumination: 50 μEinstein m^{-2} s^{-1}.

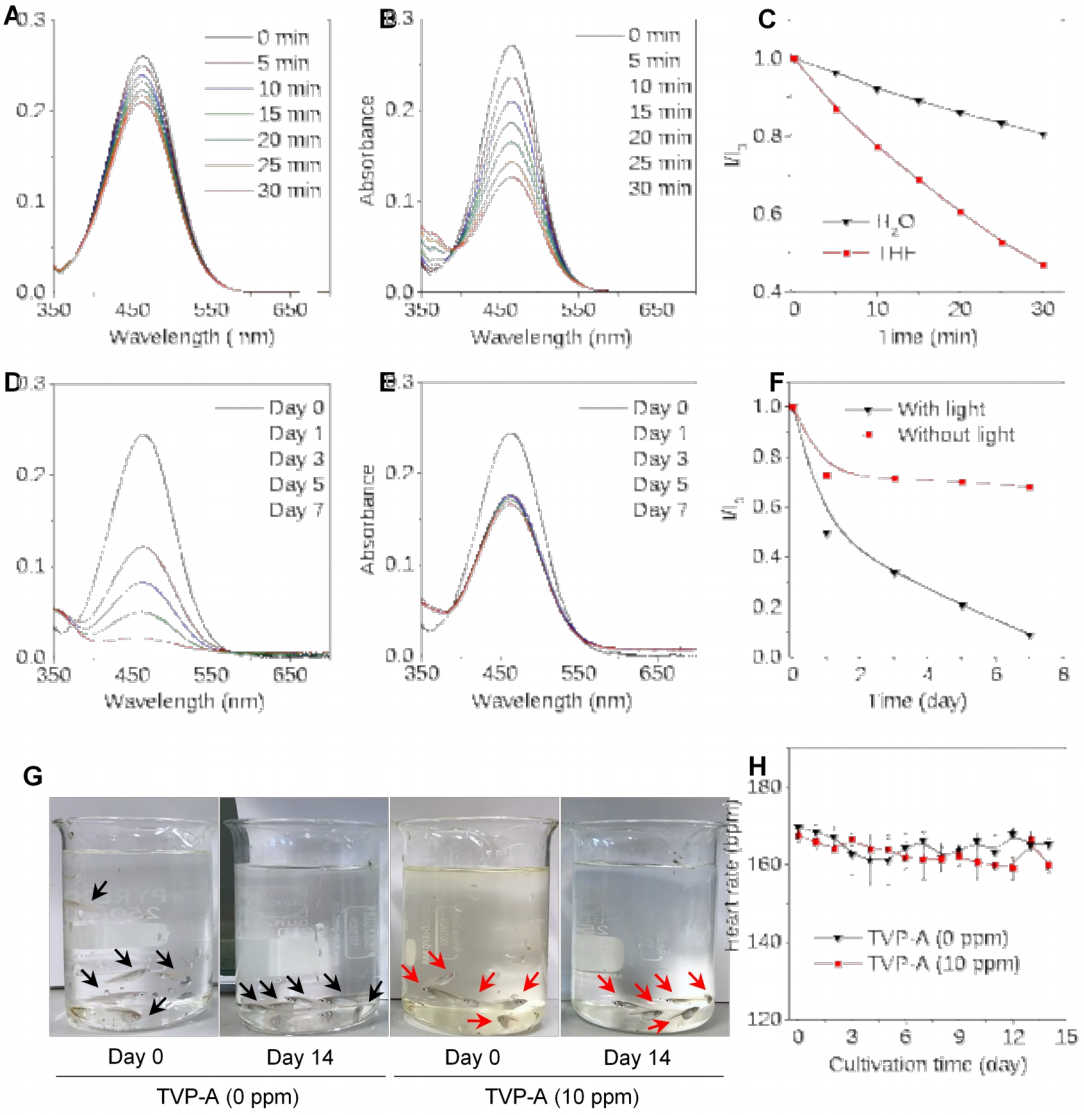

Figure 4. (A) UV/Vis absorption spectra of the TVP-A water solution (5 ppm) upon white light irradiation (350-800 nm, 10 mW cm^{-2}) for different time. (B) UV/Vis absorption spectra of the TVP-A THF solution (5 ppm) upon white light irradiation (350-800 nm, 10 mW cm^{-2}) for different time. (C) The change of relative absorbance at 462 nm in (A) and (B) as a function of white light irradiation, where I_0 is the absorbance of the corresponding solution without irradiation. (D) UV/Vis absorption spectra of the mixture of TVP-A and *C. reinhardtii* with different natural light illumination time. (E) UV/Vis absorption spectra of the mixture of TVP-A and *C. reinhardtii* kept in dark for different time. (F) The change of relative absorbance at 462 nm in (D) and (E) as a function of time. (G) Photographs of the microcosm composed of *C. reinhardtii* (5×10^4 cells mL^{-1}), *O. latipes* (5), fish bait, TVP-A (0 or 10 ppm), before and after being cultivated under 16 h light (50 μEinstein m^{-2} s^{-1})/8 h dark cycles for 14 days. (H) The change of average heart rates of the fish as a function of cultivation time.

A new AIEgen TVP-A that can control harmful algal blooms with ultra-high efficiency and no secondary pollution is designed and synthesized. TVP-A generates reactive oxygen species ultra-efficiently upon natural light irradiation, and triggers oxidative death of algal cells at extremely low concentrations. Its gradual degradation under natural light illumination also makes TVP-A friendly to ecological systems.

Keywords: harmful algal blooms, photodynamic therapy, aggregation-induced emission, photosensitizers, reactive oxygen species

Qiang Yue, Xuewen He, Neng Yan, Sidan Tian, Chenchen Liu, Wen-Xiong Wang, Liang Luo* and Ben Zhong Tang**

Title: Photodynamic Controls of Harmful Algal Blooms by an Ultraefficient and Degradable AIEgen-based Photosensitizer

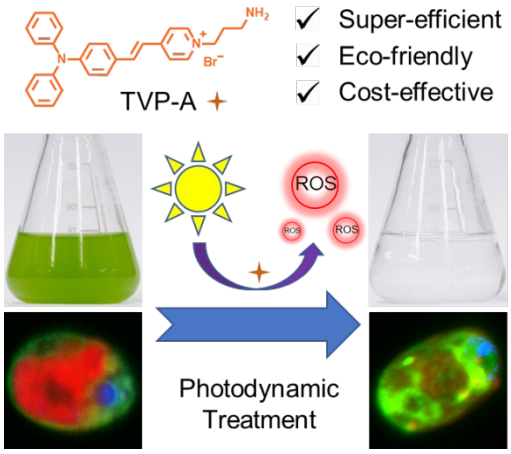

Supporting Information

Photodynamic Controls of Harmful Algal Blooms by an Ultraefficient and Degradable AIEgen-based Photosensitizer

Qiang Yue, Xuewen He, Neng Yan, Sidan Tian, Chenchen Liu, Wen-Xiong Wang, Liang Luo* and Ben Zhong Tang**

Table of Contents

1. Experimental Section.....1
1.1 Materials and Instruments.....1
1.2 Experimental Methods.....3
1.2.1 Synthesis of TVP-A.....3
1.2.2 AIE characteristics of TVP-A.....3
1.2.3 Measurement of multiple ROS generation efficiencies.....4
1.2.4 Algal culture.....5
1.2.5 Algal cytotoxicity test.....5
1.2.6 Microcosm experiment.....6
1.2.7 Zeta Potential Measurement.....7
1.2.8 SEM image of algal cells.....7
1.2.9 CLSM image of algal cells.....7
1.2.10 Monitoring the changes in autofluorescence of chlorophyll.....8
1.2.11 Degradation of TVP-A.....8
1.2.12 Mammalian cell cytotoxicity test.....9
2. Figures.....10

1. Experimental Section

1.1 Materials and Instruments

Rose Bengal lactone (RB, 95%), 2',7'-Dichlorodihydrofluorescein diacetate (DCF-DA, 97%), 9,10-Dimethylanthracene (ABDA, 99%), 3-Bromopropylamine hydrobromide, Hexamethyl Disilazane (HMDS) and 4′,6′-diamidino-2-phenylindole (DAPI) were purchased from Sigma-Aldrich and used as received. Bovine serum albumin (BSA) was purchased from Biosharp; Fetal bovine serum (FBS), Dulbecco's Modified Essential Medium (DMEM), penicillin and streptomycin were purchased

from M&C Gene Technology (Beijing) Co., Ltd. 3-(4,5-dimethyl-2-thiazolyl)-2,5-diphenyl tetrazolium bromide (MTT) was purchased from Boster Biological Teachnology Co., Ltd. Cell culture plate and 96-well plate were purchased from Guangzhou Jet Bio-Filtration Co., Ltd. Hydroxyphenyl fluorescein (HPF) and dihydrorhodamine 123 (DHR) were purchased from Thermal Fisher Scientific. The commercial algaecide Alg (anti-cyanobacteria kit Daphbio®) was purchased from Daphbio, France. 4-(N, N-diphenylamino)benzaldehyde (98%), 4-methylpyridine (98.5%), potassium tert-butoxide (99%), dichloromethane (DCM), N,N-dimethylformamide (DMF), tetrahydrofuran (THF), acetonitrile and ethyl acetate were purchased from J&K. Other compounds were purchased from AIEgen Biotech. Co., Limited. All other reagents and solvents are of analytical grade and were distilled before using.

NMR spectra were measured on a Bruker ARX 400 NMR spectrometer. Chemical shifts were reported in parts per million (ppm) referenced with respect to the residual solvent. $CDCl_3$ was used as the solvent. UV-vis absorption spectra were taken on a Milton Ray Spectronic 3000 array spectrophotometer. Fluorescence spectra were recorded on a Perkin-Elmer LS 55 spectrofluorometer. The Zeta Potential values were recorded on a Malvern Instrument Zetasizer Nano Series (Malvern Instruments, Westborough, MA, USA) equipped with a He−Ne laser (λ = 633 nm, max 5 mW) and operated at a scattering angle of 173°. Confocal laser scanning microscopy (CLSM) images were recorded on a Zeiss laser scanning confocal microscope LSM7 DUO with ZEN 2009 software (Carl Zeiss). The absorbance of MTT at 570 nm was

measured by a microplate reader (Varioskan LUX, Thermo Scientific, USA). Scanning electronic microscopy (SEM) images were recorded on a JSM-6390 (JEOL).

1.2 Experimental Methods

1.2.1 Synthesis of TVP-A

Synthesis of Compound **1** was referred to our previous report (X. He et al., *J. Am. Chem. Soc.* 2020, 142, 3959-3969). The solvent of acetonitrile (10 mL) was added to Compound **1** (200 mg, 0.58 mmol) and 3-bromopropylamine hydrobromide (190 mg, 0.87 mmol) and stirred for 1 hour at room temperature, then heated to reflux overnight. The product was precipitated out by 20 mL ethyl acetate for three times. The residue was subjected to column chromatography with alumina component, using DCM and methanol mixture (98:2, v/v) as eluent to afford TVP-A as a red solid (203.8 g, 0.42 mmol) in 72.4 % yield. 1H NMR (Bruker Avance, 400 MHz, CD_3OD), δ (ppm): 8.73-8.71 (m, 2H), 8.10 (m, 2H), 7.90 (m, 1H), 7.62-7.59 (m, 2H), 7.36-7.32 (m, 4H), 7.27-7.23 (m, 1.5H), 7.17-7.12 (m, 6H), 7.00-6.98 (m, 2.5H), 4.57-4.52 (m, 2H), 2.74-2.70 (m, 2H), 2.14-2.10 (m, 2H), 1.29 (s, 2H); 13C NMR (Bruker Avance, 100 MHz, CD_3OD), δ (ppm): 154.6, 150.5, 146.7, 143.7, 143.5, 141.7, 141.5, 129.5, 129.4, 129.2, 127.9, 125.5, 124.3, 124.2, 123.2, 123.1, 120.8, 120.7, 119.5, 57.9, 37.5, 33.7. HRMS (EI): calculated for $C_{28}H_{28}BrN_3$ $[M^-Br]^+$: 406.2278; found: 406.2301.

1.2.2 AIE characteristics of TVP-A

TVP-A was dissolved in water and then diluted with THF. The fluorescence spectra of TVP-A (5 ppm) in mixture of THF/water at various fractions of THF. TVP-A (5 ppm)

was dissolved in water, and its fluorescence spectra were recorded at various concentrations of BSA or algal cells. Fluorescence spectra were recorded on a Perkin Elmer LS 55 spectrometer.

1.2.3 Measurement of multiple ROS generation efficiencies

The total ROS, singlet oxygen ($^1O_2$), superoxide radical ($O_2^{\bullet-}$) and hydroxyl radical (•OH) generation efficiencies of TVP-A in water upon white light irradiation were determined using 2',7'-dichlorofluorescein diacetate (DCF-DA) (A. Gomes, et al., *J Biochem Biophys Methods* **2005**, *65*, 45-80), 9,10-anthracenediyl-bis(methylene) dimalonic acid (ABDA) (Y. Gao, et al., *Adv. Func. Mater.* **2019**, *29*, 1902673), dihydrorhodamine 123 (DHR) (L. M. Henderson, et al., *Eur. J. Biochem.* 1993, 217, 973-980.), 2-[6-(4-hydroxy)phenoxy-3H-xanthen-3-on-9-yl]benzoic acid (HPF) (K. Setsukinai, et al., J. *Biol. Chem.* 2003, 278, 3170-3175) as indicators respectively, and Rose Bengal (RB) as the standard reference according to previous literatures ([a] D. Wang,et al., *Adv Mater*. 2018, 30, e1802105; [b] W. Wu, et al., Adv Mater 2017, 29). The UV–vis absorption spectra of ABDA (20 μM) in TVP-A (5 ppm) or RB (5 ppm) 1× PBS aqueous solution irradiated for different durations with white light irradiation (350-800 nm, 1mW cm^{-2}) were recorded using a Milton Ray Spectronic 3000 array spectrophotometer. The fluorescence spectra of DCF-DA (10 μM), DHR (10 μM) and HPF (10 μM) in TVP-A (5 μM) or RB (5 μM) aqueous solution irradiated for different durations with white light irradiation were recorded using a Perkin Elmer LS 55 spectrometer. The absorbance of ABDA at 380 nm, and the fluorescence increase of DCF-DA at 524 nm, DHR at 525 nm as well as HPF at 513 nm were recorded upon

different irradiation time to obtain the indicators consumption rate and ROS generation efficiency.

1.2.4 Algal culture

The freshwater green algae *Chlamydomonas reinhardtii* (*C. reinhardtii*) were maintained in our laboratory for more than 20 years. *Chlorella vulgaris* (*C. vulgaris*) and *Microcystis aeruginosa* (*M. aeruginos*) were obtained from the Institute of Hydrobiology, Chinese Academy of Sciences. *C. reinhardtii* were cultured in the artificial WC (Woods Hole Chu-10) medium (R. R. L. Guillard, et al., *J. Phycol.* V8 1972) with bubbled air at 23.5 °C. We use 16 h light (50 μEinsteins m^{-2} s^{-1})/8 h dark cycle to simulate daily changes of natural light illumination and darkness. *C. vulgaris* and *M. aeruginos* were cultured in the BG11 medium (H. Song, et al., *ISME J*. 2017, 11, 1865-1876) with bubbled air at 23.5 °C under the same simulated daily cycles. All subsequent tests about algal cells were performed on the basis of the above standard culture conditions. Cells were counted under the microscope (Olympus cx31rtsf) by using a traditional hemocytometer-based method.

1.2.5 Algal cytotoxicity test

The algal cells (1.5×10^7 cells mL^{-1}) were exposed to TVP-A for 96 h at different concentrations (0, 0.2, 0.5, 1, 2.5, 5 and 10 ppm) under the simulated daily cycles. Afterwards, the cell number was measured by using the methods mentioned above, and the 96-h EC_{50} was calculated based on the toxicity test results. To investigate the effectiveness of TVP-A as potential algaecide, we tested TVP-A at different concentrations using algal cells at the stationary phase and the results were compared

with that of Alg. Specifically, *M. aeruginosa* (1.8×10^7 cells mL^{-1}), *C. reinhardtii* (1.6×10^7 cells mL^{-1}) and *C. vulgaris* (1.4×10^7 cells mL^{-1}) were respectively exposed to different concentration of TVP-A (2.5 ppm and 5 ppm) and Alg (10 ppm and 100 ppm). After different time intervals, the cell number was measured using the methods mentioned above.

To investigate the capability of TVP-A in preventing the occurrence of algal blooms, *M. aeruginosa* (5.0×10^5 cells mL^{-1}), *C. reinhardtii* (5.2×10^5 cells mL^{-1}) and *C. vulgaris* (5.0×10^5 cells mL^{-1}) were respectively exposed to TVP-A (5 ppm) and Alg (100 ppm). After different time intervals, the cell number was measured using the methods mentioned above.

1.2.6 Microcosm experiment

The microcosm, comprising of algae (phytoplankton, *C. reinhardtii*, 5.0×10^6 cells mL^{-1}) and fresh water Japanese medaka *Oryzias latipes* (Institute of Hydrobiology, Chinese Academy of Science, China, 5 per flask), was built to investigate the biocompatibility and potential environmental risk on other aquatic organisms. 10 ppm of TVP-A was added into the microcosm (250 mL), including five fish, algal cells (5×10^4 cells mL^{-1}), fish bait (Brekk. Su, Guangdong Haid Group Co., Ltd.) and filtered creek water in 250 ml flasks, and the total exposure duration was two weeks. (N. Yan, et al., *Environ. Sci. Technol.* **2019**, *53*, 5895-5905) Each day, the health of fish was evaluated by counting the heart beats. The heartbeat of the Medaka fish was recorded daily. Heart rate was measured as mean heartbeat per minute. Larvae were allowed to “rest” for roughly one minute before being measured. A hand-held counter

was used to record heartbeats for 15 seconds.

1.2.7 Zeta Potential Measurement

TVP-A (5 ppm) treated algal cells (*C. reinhardtii*, 5.0×10^6 cells mL^{-1}) in the artificial WC medium were exposed to the simulated natural light (50 μEinsteins m^{-2} s^{-1}) for 0, 10, 30, 60 min. Then algal samples were washed with artificial WC medium by centrifugation (2000 rpm, 3 min) for three times for final detection.

1.2.8 SEM image of algal cells

The algal cells (*C. reinhardtii*, 5.0×10^6 cells mL^{-1}) were co-incubated with TVP-A (5ppm) in the artificial WC medium under the simulated natural light illumination (50 μEinsteins m^{-2} s^{-1}) for 2 hours. The samples were then washed with the artificial WC medium by centrifugation (2000 rpm, 3 min) three times. The algal samples were then placed in 1% glutaraldehyde in the artificial WC medium overnight at 4 °C. The samples were then washed with 0.1 M phosphate buffer solution (PBS, pH 7.4) by centrifugation (2000 rpm, 3 min) three times. Next, algal samples were dehydrated successively through a series of alcohol solutions of 30%, 50%, 70%, 80%, 90%, 95% and 100% for 15 min. After dehydration, samples were fixed with Hexamethyl Disilazane (HMDS) and then freeze-dried for 6 hours. Finally, algal samples were sprayed with gold for observation. (C. Zhang, et al., *Environ. Pollut* 2017, 220, 1282-1288)

1.2.9 CLSM image of algal cells

The algal cells (*C. reinhardtii*, 5.0×10^6 cells mL^{-1}) were co-incubated with TVP-A (5ppm) in the artificial WC medium under the simulated natural light illumination (50

μEinsteins m^{-2} s^{-1}) for various irradiation time. The samples were then washed with the artificial WC medium by centrifugation (2000 rpm, 3 min) three times. Then algal samples were placed in 1% glutaraldehyde in for 10 min. The algal cells were then treated with DAPI for 10 min following wash and centrifugation for 3 times. The Algal samples were finally transferred to confocal dish for observation Conditions: for TVP-A, excitation wavelength: 488 nm, emission filter: 570-630 nm; for DAPI, excitation wavelength: 405 nm, emission filter: 450-500 nm; for chlorophyll, excitation wavelength: 405 nm, emission filter: 679-700 nm.

1.2.10 Monitoring the changes in autofluorescence of chlorophyll

C. reinhardtii (1.6×10^7 cells mL^{-1}) were treated with TVP-A (5 ppm) and cultured in beakers (100 mL) under the simulated natural light (50 μEinsteins m^{-2} s^{-1}). Each 3 mL of algal suspension was removed from the medium and transferred to a cuvette, upon different irradiation times, for fluorescence measurement (λ_{ex} = 405 nm, λ_{em} = 500-800 nm).

1.2.11 Degradation of TVP-A

The degradation of TVP-A upon photooxidation: TVP-A was dissolved in water or dispersed in THF by ultrasound (5 ppm), and then exposed to white light (350-800 nm, 10 mW cm^{-2}) irradiation. The absorbance spectra of TVP-A aqueous solution and THF solution upon different irradiation time.

The degradation of TVP during algal bloom government: *C. reinhardtii* (5×10^6 cells mL^{-1}) were co-incubated with TVP-A (5 ppm) in beakers (100 mL), followed by being exposed to simulated natural light (50 μEinsteins m^{-2} s^{-1}) or kept in darkness during a

week. Each 3 mL algal suspension was removed daily from the medium and transferred to a cuvette for the absorption spectrum measurement of TVP-A.

1.2.12 Mammalian cell cytotoxicity test

Human umbilical cord vein endothelial cells (HUVEC) were kindly obtained from Tongji Medical College, Huazhong University of Science and Technology). HUVEC cells (10000 cells mL^{-1}) were seeded in 96-well plates and cultured in the DMEM containing 10% FBS and 1% antibiotics (10000 units mL^{-1} penicillin and 10 mg mL^{-1} streptomycin) in a 5% CO_2 humidity incubator at 37 ℃ for 24 h. The cells were then incubated with TVP-A at various concentrations (0, 0.5, 1, 2, 4, 8, 16 ppm) in the dark for another 24 h, and then 10 μL of freshly prepared MTT (5 mg mL^{-1}) solution was added into each well. The MTT solution was carefully removed after 3 h of incubation, and DMSO (120 μL) was added into each well to dissolve all the formazan formed. Cell viability was expressed by the ratio of the absorbance (at 570 nm) of MTT in the cells incubated with TVP-A to that of in the cells incubated with culture normal medium.

2. Figures

Figure S1. Synthetic route to TVP-A.

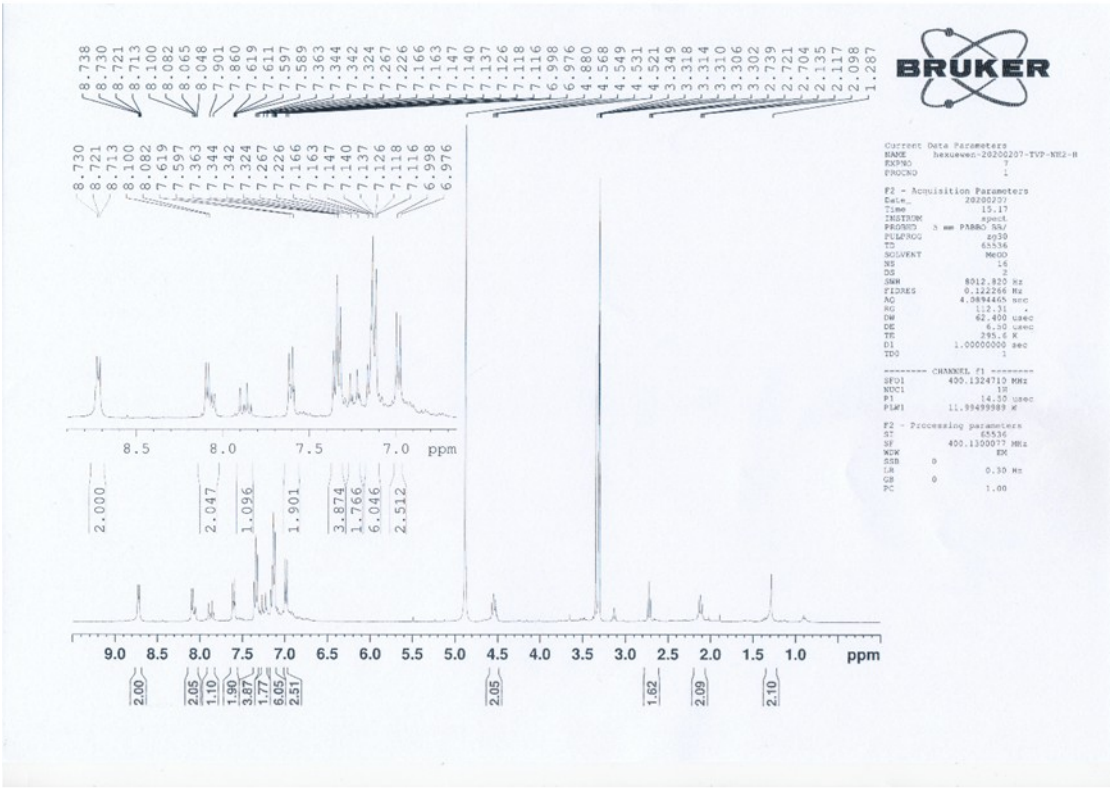

Figure S2. ^{1}H NMR spectrum of TVP-A in CD_3OD.

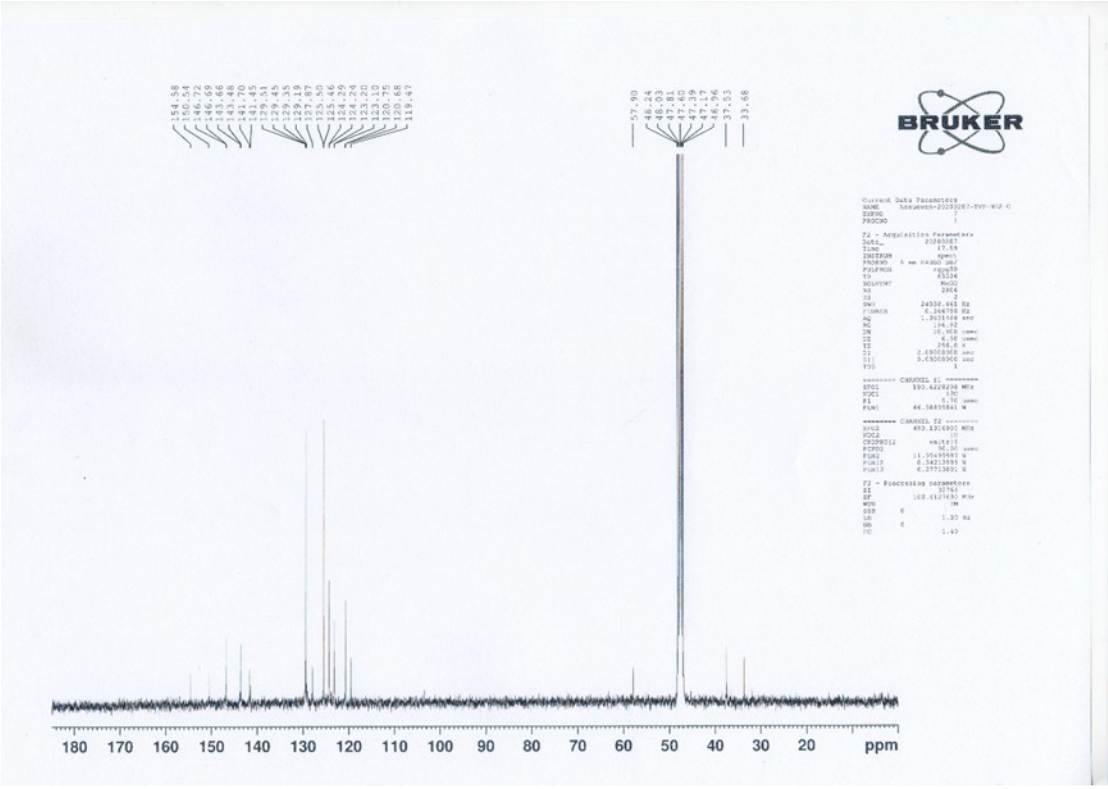

Figure S3. ^{13}C NMR spectrum of TVP-A in CD_3OD.

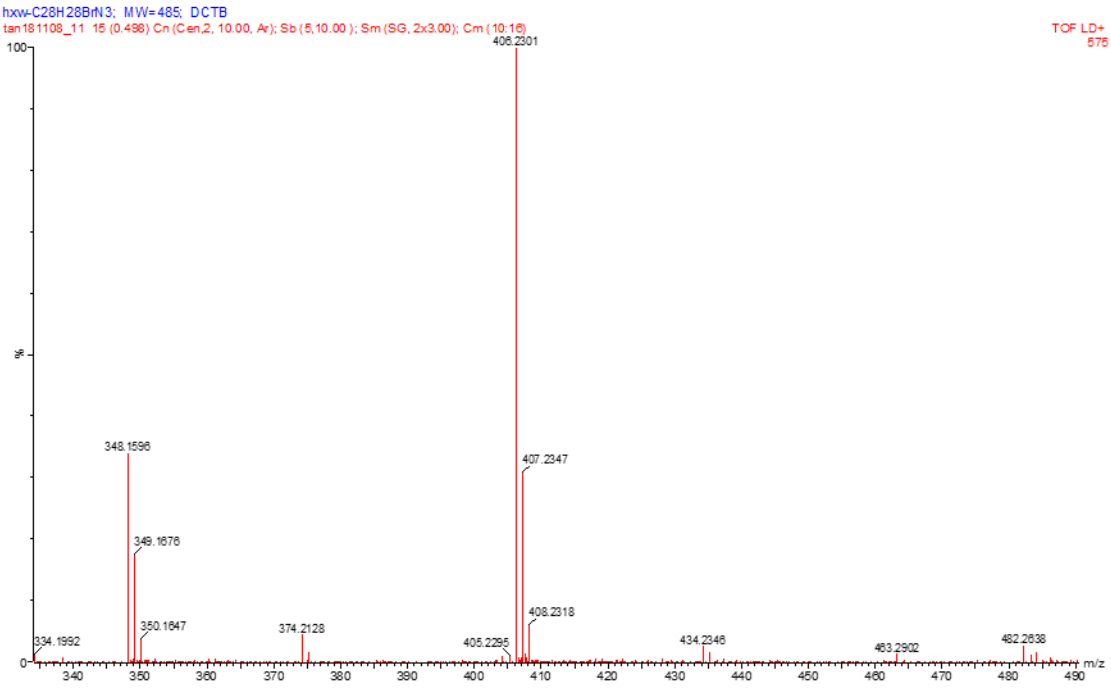

Figure S4. High resolution mass spectrum of TVP-A.

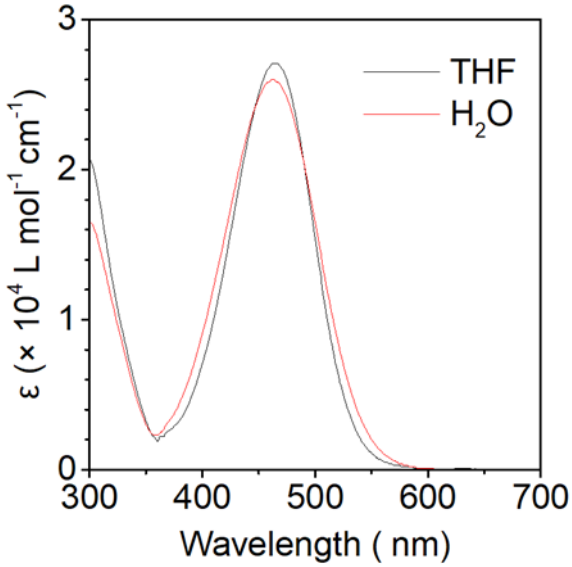

Figure S5. A) The Molar Absorption Coefficient (ε) of TVP-A (10^{-5} mol L^{-1}) dissolved in H_2O or dispersed in THF.

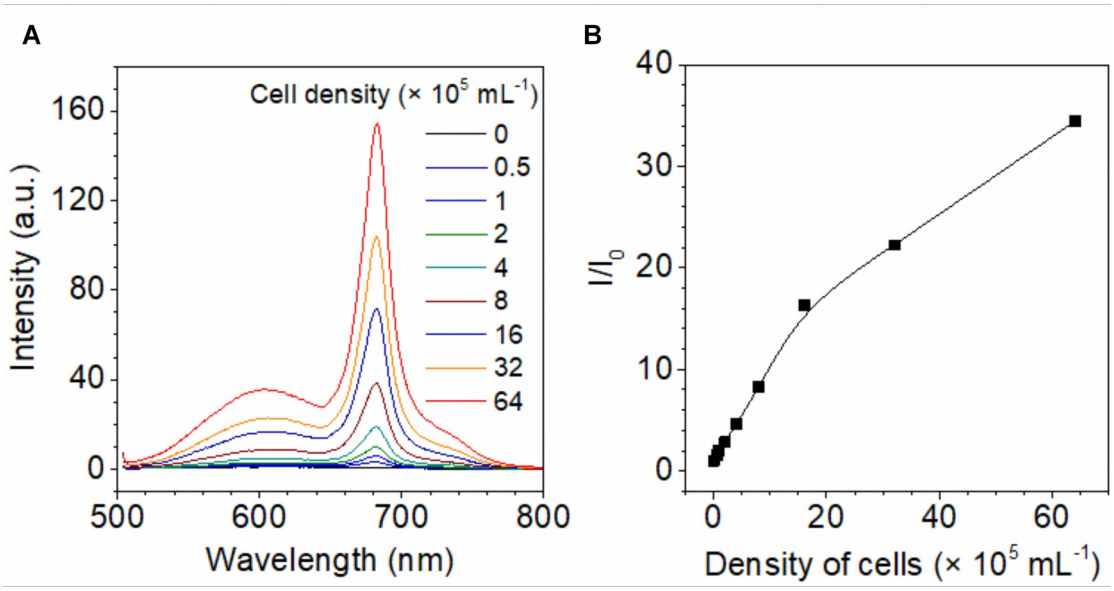

Figure S6. A) The fluorescence spectra of TVP-A aqueous solutions added with varying density of algal cells (*C. reinhardtii)*. B) FL intensity at 605 nm as a function of the density of algal cells.

Conditions for Q.Y. Measurement	Q.Y. (%)
H2O	0.27±0.05
DMSO	1.27±0.05
THF	11.6±0.24
$CHCl_3$	18.93±0.05
BSA aqueous solution	30.73±0.05

Table S1. Fluorescence quantum yields of TVP-A under different solvent or solution conditions.

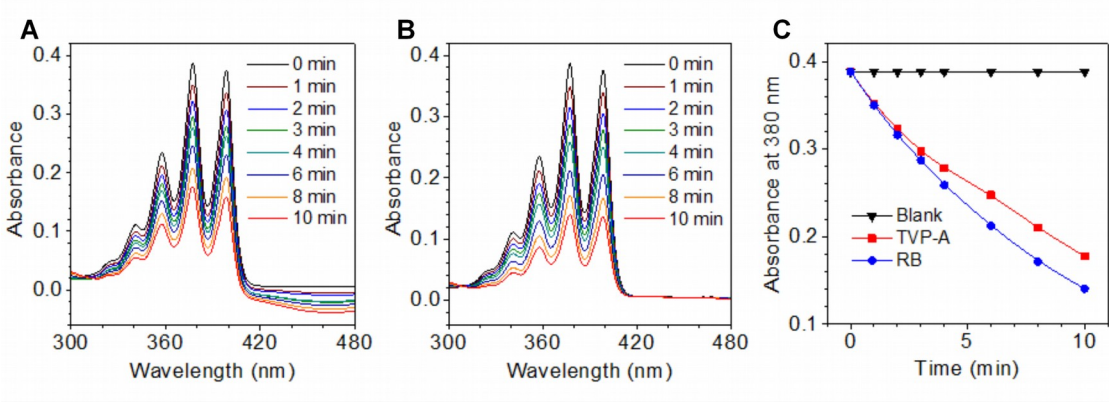

Figure S7. UV–vis absorption spectra of ABDA (20 μM) in A) TVP-A (5 ppm) aqueous solution and Rose Bengal (RB, 5 ppm) aqueous solutions irradiated for different durations with white light irradiation (350-800 nm, 1 mW cm^{-2}). C) Absorbance of ABDA at 380 nm in Blank, TVP-A (5 ppm), and Rose Bengal (RB, 5 ppm) aqueous solutions for different durations with white light irradiation (350-800 nm, 1 mW cm^{-2}).

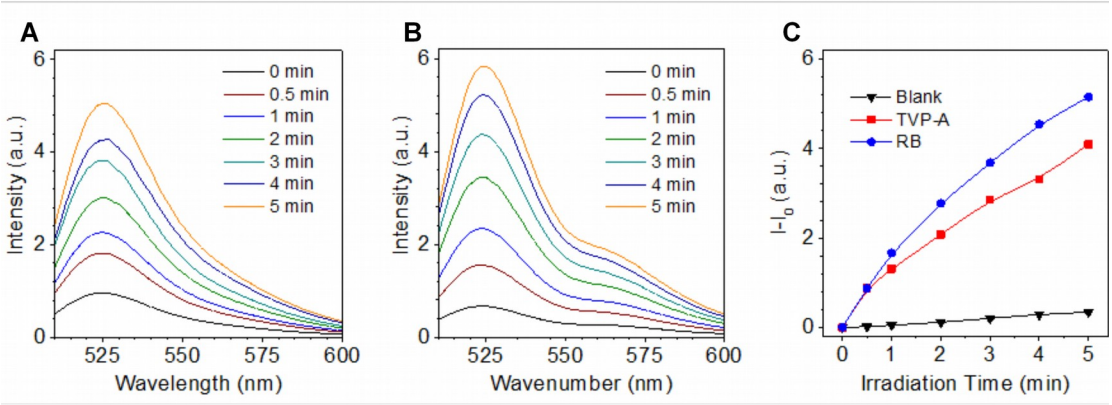

Figure S8. Fluorescence spectra of DHR (10 μM, λ_{ex} = 500 nm) in (A) TVP-A (5 ppm) aqueous solution and (B) Rose Bengal (RB, 5 ppm) aqueous solutions irradiated for different durations with white light irradiation (350-800 nm, 1 mW cm^{-2}). C) Intensity of DHR at 525 nm in Blank, TVP-A (5 ppm), and Rose Bengal (RB, 5 ppm) aqueous solutions for different durations with white light irradiation (350-800 nm, 1 mW cm^{-2}).

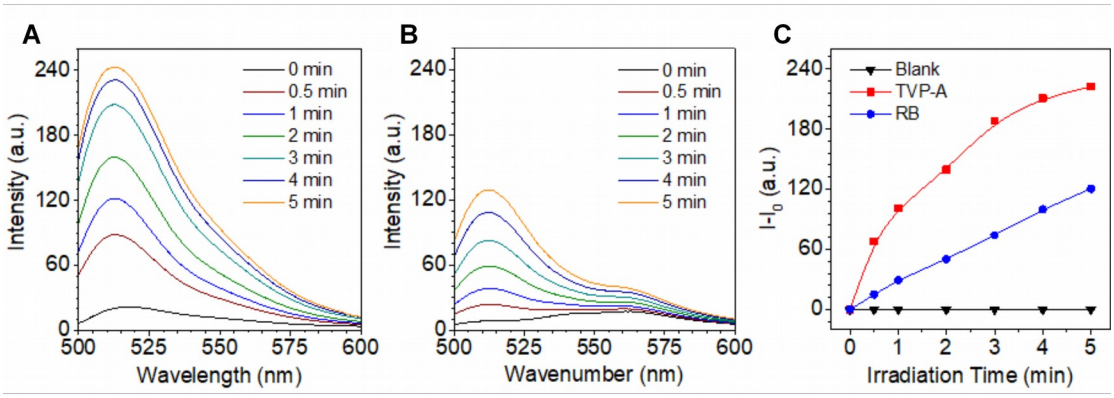

Figure S9. Fluorescence spectrum of HPF (10 μM, λ_{ex} = 488 nm) in (A) TVP-A (5 ppm) aqueous solution and (B) Rose Bengal (RB, 5 ppm) aqueous solutions irradiated for different durations with white light irradiation (350-800 nm, 1 mW cm^{-2}). (C) Intensity of HPF at 513 nm in Blank, TVP-A (5 ppm), and Rose Bengal (RB, 5 ppm) aqueous solutions for different durations with white light irradiation (350-800 nm, 1 mW cm^{-2}).

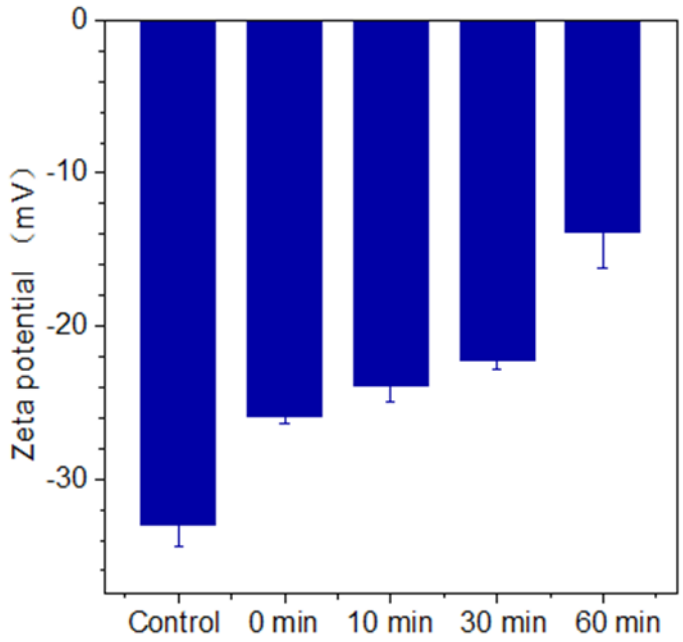

Figure S10. Zeta potential measurements for TVP-A treated and untreated algal cells (*C. reinhardtii*), and the change in zeta potential following TVP-A incubation.

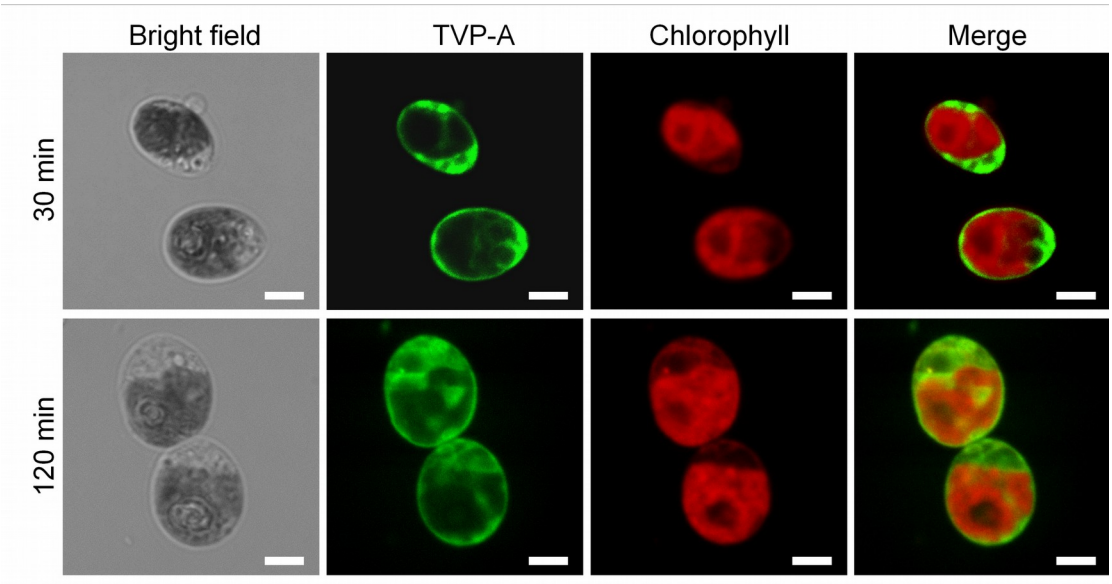

Figure S11. CLSM images of a *C. reinhardtii* cell co-incubated with TVP-A under dark conditions for 30 min (A) and 120 min (B). Scale bar: 3 μm. TVP-A: green channel, λ_{ex} = 488 nm, λ_{em} = 570–630 nm. Chlorophyll: red channel, λ_{ex} = 405 nm, λ_{em} = 670–700 nm.

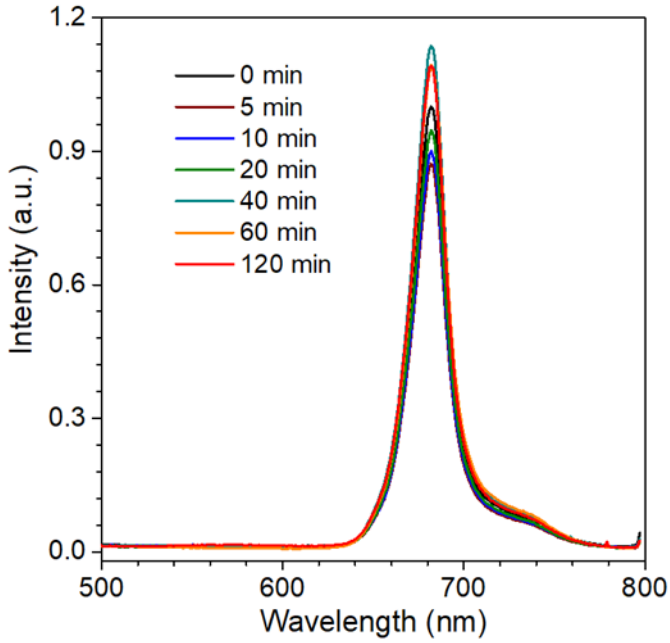

Figure S12. Fluorescence spectra of chlorophyll in algal cells (*C. reinhardtii*) with different time of simulated natural light irradiation (50 μEinsteins m^{-2} s^{-1}).

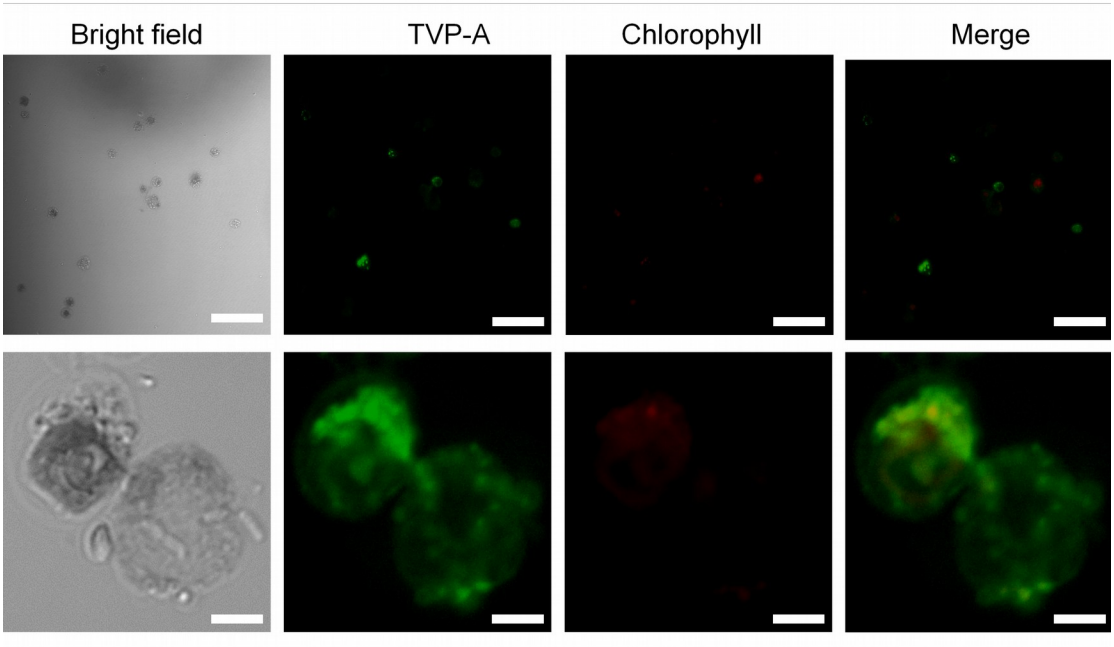

Figure S13. CLSM image of TVP-A treated algal cells (*C. reinhardtii*) exposed to simulated natural light (50 μEinsteins m^{-2} s^{-1}) for 2 min and switched to darkness for

24 hours. Scale bar: 40 μm (top row) and 3 μm (bottom row).

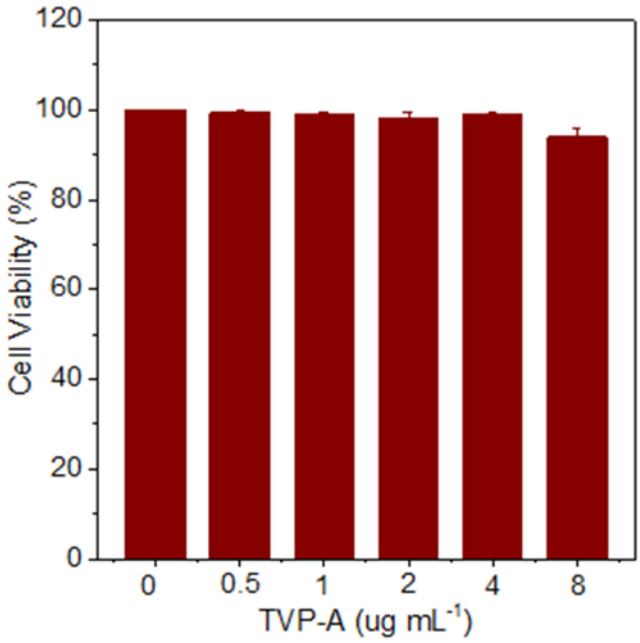

Figure S14. Dose-dependent effects of TVP-A on HUVEC cells in dark condition.